Volume 12
Number 44
28 November 2021
Pages 6365-6486

Polymer Chemistry

rsc.li/polymers

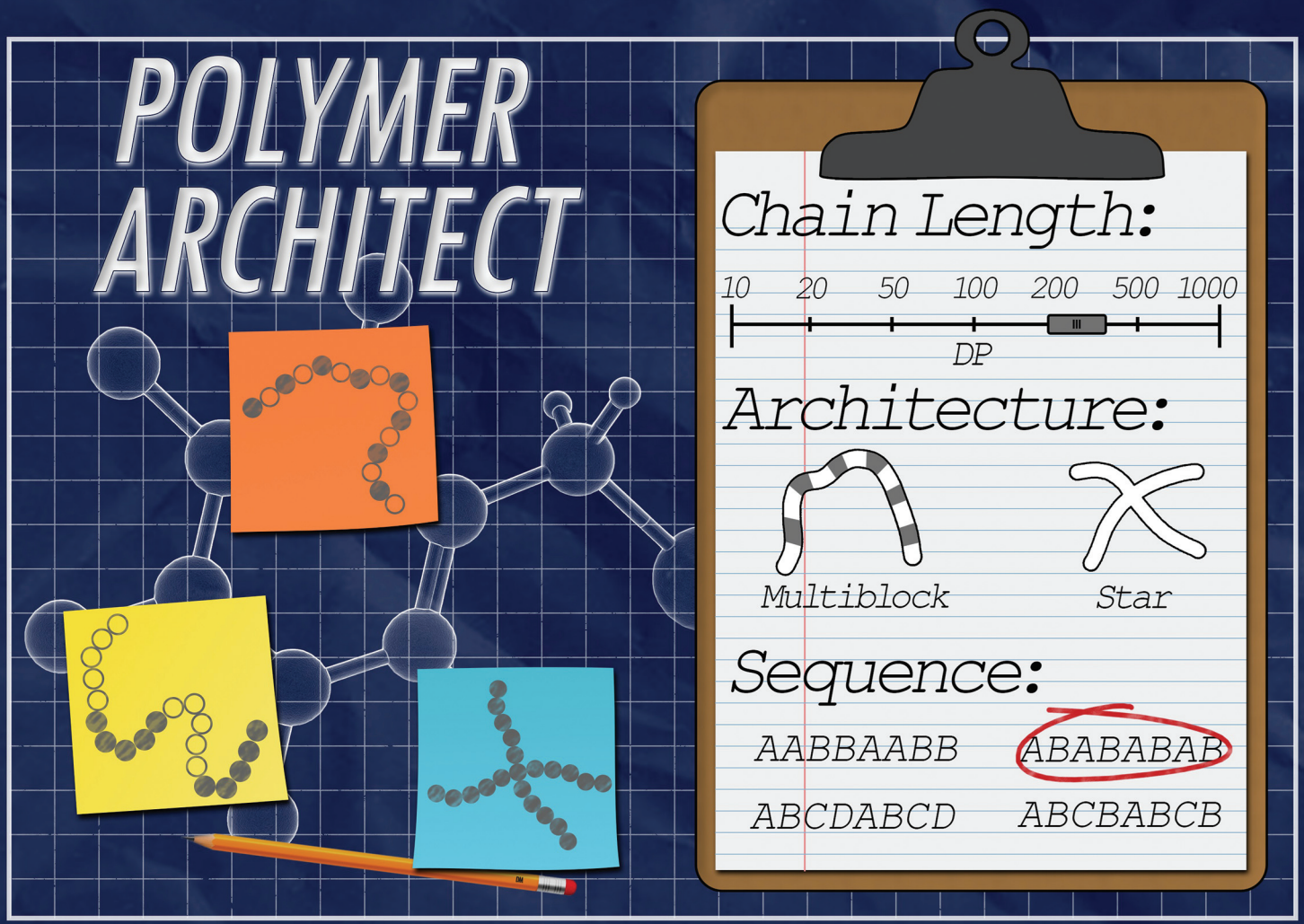

ISSN 1759-9962

ROYAL SOCIETY OF CHEMISTRY

PAPER
C. Remzi Becer *et al.*
One-pot synthesis of amphiphilic multiblock poly(2-oxazoline)s *via para*-fluoro-thiol click reactions

Polymer Chemistry

ROYAL SOCIETY OF CHEMISTRY

PAPER

View Article Online
View Journal | View Issue

Check for updates

Cite this: *Polym. Chem.*, 2021, **12**, 6392

One-pot synthesis of amphiphilic multiblock poly(2-oxazoline)s *via para*-fluoro-thiol click reactions†

Tieshuai Zhao, Ben Drain, Gokhan Yilmaz and C. Remzi Becer *

Received 12th July 2021,
Accepted 20th September 2021

DOI: 10.1039/d1py00944c

rsc.li/polymers

A clickable initiator, pentafluoro benzyl bromide, has been investigated for the cationic ring opening polymerization of poly(2-oxazolines). Additionally, the clickable alpha end group was then utilized in a *para*-fluoro-thiol click reaction to synthesise linear diblock, tetrablock, multiblock copolymers as well as star shaped poly(2-oxazoline)s using dithiol compounds as terminating agents. Thus, a one-pot approach combining the *para*-fluoro-thiol click reaction and direct termination of the poly(2-oxazoline) living chain end with 4,4-thiobisbenzenethiol has been performed to prepare multiblock copolymers of poly(2-ethyl-2-oxazoline) (PEtOx) and poly((2-ethyl-2-oxazoline)-*b*-(2-methyl-2-oxazoline) (PEtOx-*mb*-PMeOx). All obtained polymers were characterized by Size Exclusion Chromatography (SEC), ^{1}H Nuclear Magnetic Resonance (NMR) and Matrix-Assisted Laser Desorption/Ionization-Time of Flight (MALDI-ToF) mass spectrometry. Last but not least, the self-assembly properties of prepared amphiphilic polymers were studied with DLS and TEM. Nanoparticles with a diameter ranging from 184 nm to 250 nm were observed in TEM for PEtOx-*mb*-PMeOx copolymers.

Introduction

Poly(2-oxazoline)s(POx) have attracted great attention as they possess various properties including biocompatibility,[1–8] thermal responsive ability,[9–12] tunable hydrophilicity[9,13] and adjustable cytotoxicity[7,14,15] that are useful for biomedical and industrial applications such as adhesives[10] and lubricants.[16] Synthesis of poly(2-oxazoline)s with well-defined chain length, and end groups has been achieved through a living cationic ring-opening polymerization (CROP) process that can be initiated by various commercially available initiators such as tosylates, triflates, acid halides, and benzyl halides.[17] Thus, the living chain ends have been further utilized in chain extension reactions to obtain block copolymers[10,13,18,19] or alternatively have been functionalized to introduce functional groups for post-polymerization modification (PPM) reactions.[20–22]

Owing to the biocompatibility of POx, synthesis of poly(2-oxazoline) based block copolymers with amphiphilic structures to form polymeric micelles or nanoparticles have been on the focus of many research groups.[23–28] Preparation of diblock, triblock and tetrablock POx and subsequent manufacturing of micelles and nanoparticles have been already reported.[10,12,13,18,29–31] There are two main methods for the synthesis of 2-oxazoline based block copolymers. These methods are sequential addition of monomers to the polymerization mixture after complete consumption of the previous monomer, and the coupling of end-functionalized polymers[11] (Scheme 1A). The former method (aka sequential addition method) was the most widely employed one since one-pot process is more convenient to obtain multiblock polymers.[32] However, the chain length of block polymers synthesized *via* this method is relatively limited due to decreased chain end fidelity and the steric hinderance of the living chain end at high molar mass.[17] The later method (aka polymer–polymer coupling method) allow combination of more diverse backbone functionalities into POx block copolymer structures[33,34] (Scheme 1B). For instance, POx polymers were synthesized and end-capped with functional groups (*i.e.* sodium azide, amines, thiols, and carboxylic acids) for subsequent coupling with mainly vinyl polymers.[35–37] However, the overall efficiency of the subsequent polymer–polymer coupling reaction is limited by nature of the reactivity of the chemical groups and the steric hinderance caused by the folding of the polymer chain that can significantly limit the accessibility of functional groups on the α- and ω-terminal of POxs.

Click reactions are known to be highly efficient reactions that require mild conditions to give high yields.[38,39] These properties make click reactions good candidates for step-growth polymerization and polymer–polymer conjugation reactions. For example, copper(I) catalyzed azide–alkyne cycloaddition (CuAAc) click reaction has been utilized in the modification and

Department of Chemistry, University of Warwick, CV4 7AL Coventry, UK.
E-mail: remzi.becer@warwick.ac.uk

†Electronic supplementary information (ESI) available: Further SEC, NMR and MALDI-ToF MS analysis of polymers can be found in the ESI. See DOI: 10.1039/d1py00944c

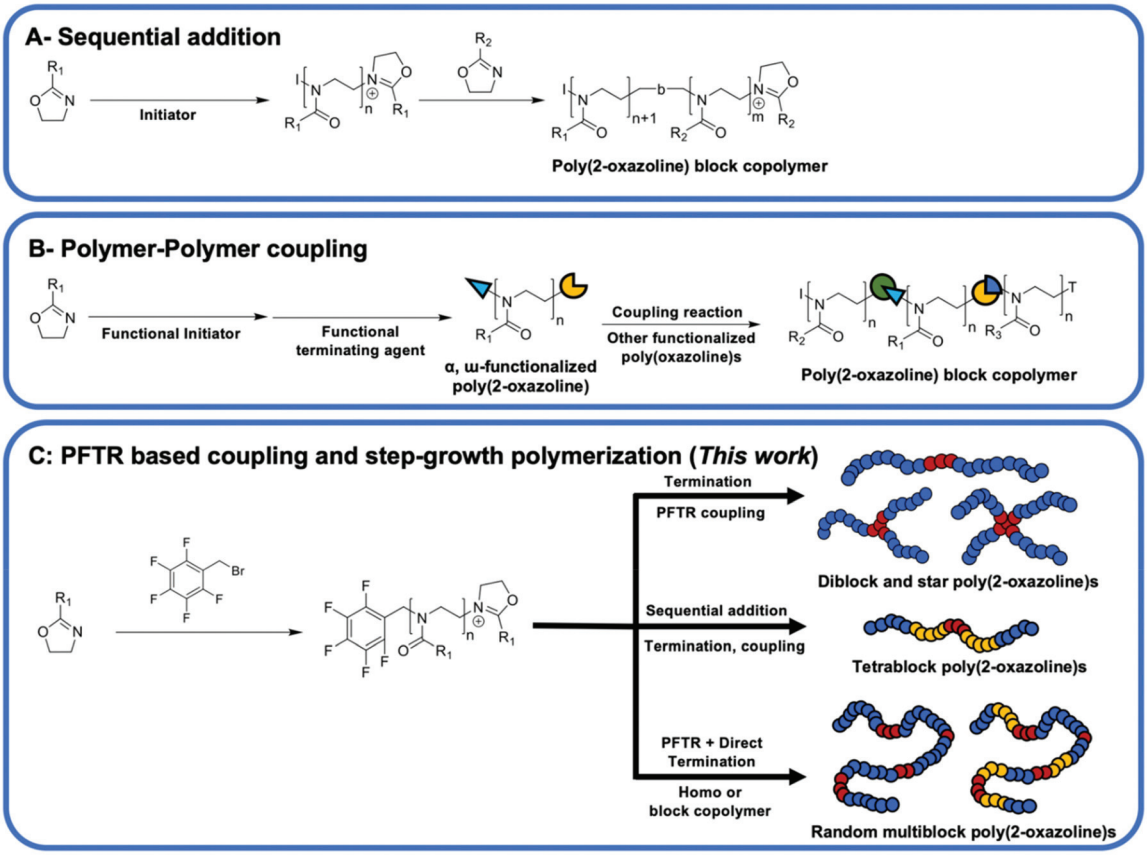

Scheme 1 Synthetic approaches to prepare poly(2-oxazoline) based block copolymers.

synthesis of block copolymers and dendrimers of POxs.[11,40,41] The clickable azide or alkyne groups are introduced through the use of a functional initiator[42] or by termination[43] of the living cationic chain end to prepare functionalized POx chains and subsequently reacted with other polymers to prepare linear diblock,[13,18,44] linear triblock,[10] and star shaped polymers.[42] However, the undesired strong interaction between amide groups on POx backbone and Cu catalyst creates a real challenge in the purification of the final product.[45]

Utilizing metal-free click reactions such as thiol–ene reaction[46] and Cu-free strain-promoted azide–alkyne cycloaddition (SPAAC) click reactions[47] to synthesize block copolymers have also been reported. Besides, studies on α- and ω-terminal functionalized POxs usually led to synthesis of diblock copolymer or triblock copolymer due to low coupling efficiency of POxs,[17,22] while the selected polymer–polymer coupling reaction utilized in reports was mainly CuAAc click reaction[13,18] with some studies employed thiol-based click reactions to prepare star, grafted and block copolymer of POxs.[48–50] The use of *para*-fluoro-thiol click reaction to prepare POx block copolymers was not reported. Additionally, research on the synthesis of multiblock POxs using a difunctionalized POx precursor *via* a step growth approach remains absent (Scheme 1C).

Herein, we introduce the use of pentafluoro benzyl bromide (PFBB) as a functional initiator for the CROP of poly(2-ethyl-2-oxazoline) (PEtOx). Clickable functionality allows the preparation of linear diblock, star shaped and multiblock poly(2-oxazolines). Utilizing commercially available dithiol and multithiol compounds, linear diblock and star shaped polymers of PEtOx were synthesized *via para*-fluoro-thiol click reaction (PFTR) approach. The block copolymer consists of 2-ethyl-2-oxazoline and 2-methyl-2-oxazoline (MeOx) was also prepared using PFBB as an initiator, and this resulted in a tetrablock copolymer of P(EtOx-*b*-MeOx) with a dithiol compound in between the blocks. Furthermore, a combination of the PFTR and direct termination of the cationic chain end of PEtOx or P(EtOx-*b*-MeOx) with dithiol as the nucleophile gives rise to a multiblock poly(2-oxazoline)s within 10 minutes in a one-pot reaction. The synthesized diblock and multiblock poly(2-oxazoline)s have presented amphiphilic structures and therefore the self-assembly properties of these polymers were investigated using transmission electron microscopy (TEM).

Results and discussion

Kinetics investigation of PFBB initiated CROP of EtOx

Kinetics investigation of the CROP of 2-ethyl-2-oxazoline (EtOx) using PFBB as an initiator was performed to establish the feasibility of using PFBB as a clickable initiator as well as to

understand the polymerization kinetics. Initial reaction conditions were used a [EtOX]:[PFBB] ratio of 60:1, giving a theoretical degree of polymerization (DP) of 60. The polymerization was performed in a microwave reactor at 140 °C, at a monomer concentration of 4.0 M, and using dry acetonitrile (MeCN) as the solvent. These conditions were widely employed in other kinetic investigations for the CROP of 2-oxazolines with other commercially available initiators such as methyl tosylate,[51] benzyl bromide,[52] and acyl halides.[53] This allowed a direct comparison of the results including rate constant of polymerization to previously reported values. A stock solution of EtOx and PFBB in dry MeCN at 4.0 M concentration was prepared and equal amounts of stock solution were distributed into a series of 2–5 mL microwave vials under inert and anhydrous conditions. These vials were then transferred to the microwave reactor, heated to 140 °C, and quenched with a sodium hydroxide/methanol solution at predetermined time points. ^{1}H NMR and SEC analysis were conducted to determine the monomer conversion, the molar mass of obtained polymers at different time points as well as the polymerization rate constant (Fig. 1). Monomer conversion was calculated based on integration of EtOx peaks in the ^{1}H NMR (ESI, Fig. S1†). ^{1}H NMR spectrum collected at each time point are shown in Fig. S1.† ^{1}H NMR results show the shift and split of the peak for the methylene group of pentafluoro benzyl bromide and the consumption of EtOx.

The plot of $\ln([M]_0/[M]_t)$ *versus* time depicted in Fig. 1A show a pseudo-linear relationship indicating that the concentration of active and propagating chains is constant throughout the polymerization. However, closer inspection of data points suggesting a slightly sigmoidal shape, which indicates the slight existence of possible slow initiation and termination. Nevertheless, the semi-logarithmic kinetic plot together with the SEC results demonstrates the living character of the polymer chains under these reaction conditions. In addition to this, the reaction time *vs.* conversion plot in Fig. 1B showing the linear dependence at low conversion, and the $M_{n,SEC}$ *vs.* conversion plot depicted in Fig. 1C shows a linear dependence further confirming a living, controlled chain growth polymerization and absence of termination or chain transfer reactions. Dispersity values were below 1.20 throughout the kinetics investigation, indicating the polymerization has proceeded in a controlled fashion. The decreasing trend of dispersity values with increasing molecular weight also fits the theoretical trend for living polymerization.[54] The linear trends in both Fig. 1A and 1C are in good agreement with experimental data with R^2 values over 0.99 were obtained. The retention time change in Fig. 1D together with the $M_{n,SEC}$ values indicated the growing character of the polymer chain, while the experimental $M_{n,SEC}$ value has stayed lower than the theoretical value. For example, at t = 12 min where the monomer conversion was around 93%, the $M_{n,Theo}$ value was 5700 Da, while the measured $M_{n,SEC}$ was only 5000 Da. This slight difference may be due to the PMMA calibration standards or due to effect of pentafluoro benzyl initiating group on overall hydrodynamic volume of the polymer.

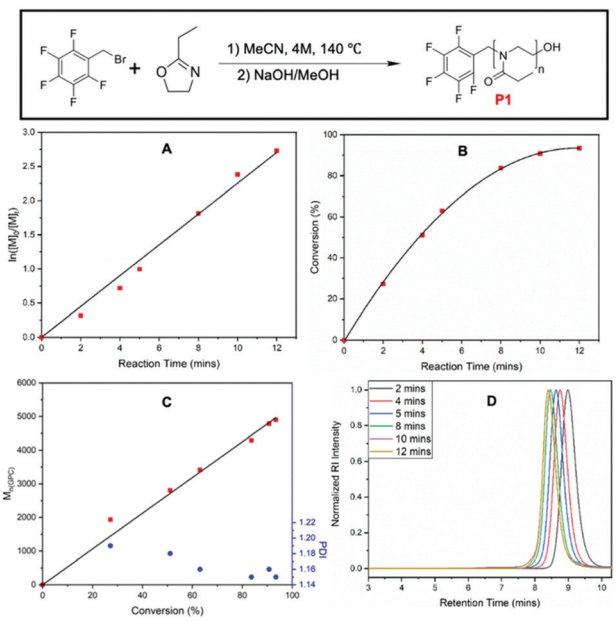

Fig. 1 Kinetics investigation of PFBB initiated CROP of EtOx. (A) Ln $([M]_0/[M]_t)$ *versus* reaction time plot, (B) Monomer conversion *versus* reaction time plot, (C) $M_{n,\,SEC}$ *versus* monomer conversion and $Đ$ *versus* monomer conversion plot, and (D) SEC monitored hydrodynamic volume change through the kinetics investigation.

The apparent propagation rate of polymerization (k_{app}) was determined based on the first order kinetics following (ESI, eqn (S2)†). While based on the assumption of concentration of initiator and living propagating chain ends are equal and given concentration of initiator at t_0 is ($[I]_0$), k_{app} was calculated as 3.38×10^{-3} L (mol s^{-1}). This kinetic study has shown that PFBB is an excellent initiator for CROP of EtOx, although the reaction rate is rather slow compared to benzyl bromide, which was reported by Schubert *et al.* as 1.14×10^{-1} L (mol s^{-1}) at 160 °C.[51] As the counter ion in each initiating system remains the same, possible reason for a moderate polymerization rate could be the pentafluoro benzyl group is more electron withdrawing and sterically large than a benzyl group, which makes the cationic species generated in initiation and propagation more energetically unfavorable.

Before exploitation of the clickable pentafluoro benzyl group on PEtOx, further investigation on the chain end nature of obtained polymers was necessary. PEtOx with a lower DP was prepared in order to ease the characterization with MALDI-ToF MS and to allow more accurate ^{1}H NMR integration analysis to calculate the initiator efficiency. PEtOx with DP 10 was synthesized using PFBB as the initiator and the polymerization was terminated with sodium hydroxide in methanol to provide hydroxyl end groups. The obtained PFB-PEtOx, which has a pentafluoro benzyl (PFB) group at the α-end of polymer, was purified and characterized with SEC, ^{1}H NMR and MALDI-ToF MS (Fig. 2). The SEC results, $M_{n,SEC}$ = 1200 Da, in Fig. 2A show a good agreement with theoretical molar mass of DP 10 PEtOx with a PFBB initiator, which is 1172.3 Da. In the MALDI-ToF spectrum shown in Fig. 2B, a

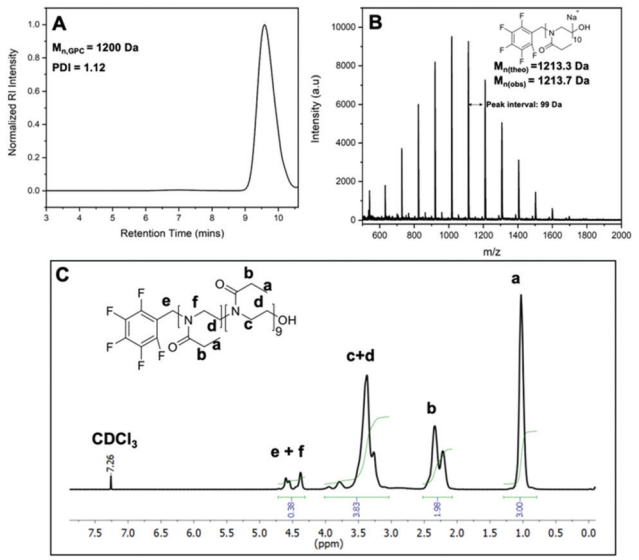

Fig. 2 (A) SEC measurement in THF as an eluent, (B) MALDI-ToF MS, and (C) ^{1}H NMR analysis of PFB-PEtOx$_{10}$. The SEC trace and the distribution shown in MALDI-ToF indicates a DP10 polymer. In the ^{1}H NMR, corresponding peaks were labelled, and part of the backbone hydrogens (**f**) shifted to lower field at around 4.5 ppm from **c+d** at 3.45 ppm due to initiating group effect.

major distribution that fits to the theoretical molar mass value of PEtOx with pentafluoro benzyl and hydroxyl end groups was observed. For instance, the observed peak at 1113.9 Da was close to the theoretical calculations of the sodium salt of PEtOx with 9 repeat units and possessing -OH and PFB end groups. Similarly, the peak at 1213.7 Da was close to the same structure with 10 repeat units and the distance between the peaks was 99 Da, which is equal to the molar mass of EtOx. It should be noted that in the ^{1}H NMR analysis the total integration ratio of peaks was 9.2. This corresponds to 90 protons of ethyl groups and 2 protons of methylene group from the initiator, which is in good agreement with a degree of polymerization of 10. However, the integration ratio of peaks from 4.2 to 4.7 ppm to the side chain methyl group (peak a, Fig. 2C) does not fit the theoretical ratio of 1 : 15. That is because of the two backbone hydrogens closest to the α-end of polymer has split from the main peak c in Fig. 2C and move towards larger chemical shift (peak f Fig. 2C). Peaks from 4.2 to 4.7 ppm include peak **e** from the initiator methylene group and peak f from the closest backbone methylene group.

Synthesis of extended linear and star shaped polymers via PFTR click reaction

As reported in our earlier work, PFTR click reaction can be utilized in preparation of step growth polymers with PFBB and dithiol compounds.[55] Thus, it is natural to investigate the possibility of using this highly efficient coupling strategy to synthesize extended linear, tetra-block and star shaped polymers of EtOx and MeOx utilizing various dithiol and multithiol compounds.

Table 1 List of polymers, their architectures and molar mass data

No	Polymer name	Architecture	$M_{n,SEC}$ (Da)	$Đ$
P1	P(EtOx)$_{10}$	Linear	1200	1.12
P2	P(EtOx$_{10}$)-**A***-P(EtOx$_{10}$)	Extended linear	2200	1.21
P3	P(EtOx$_{10}$)-**B***-P(EtOx$_{10}$)	Extended linear	2300	1.23
P4	P(EtOx$_{10}$)-**C***-P(EtOx$_{10}$)	Extended linear	2100	1.20
P5	**D***-P(EtOx$_{10}$)$_3$	3-Arm star	2900	1.41
P6	**E***-P(EtOx$_{10}$)$_4$	4-Arm star	3200	1.60
P7	P[(EtOx)$_5$-*b*-(MeOx$_5$)]	Sequential diblock	1100	1.21
P8	P7-**A**-P7	Tetrablock	2000	1.24
P9	**A**-P(EtOx)-**A**	Extended multiblock	8300	2.64
P10	**A**-P[(EtOx)-*mb*-(MeOx)]-**A**	Multiblock	4100	1.32

*A: 4,4- Thiobisbenzenethiol; **B**: 2,2′ (ethylenedioxy)diethanethiol; **C**: 1,2-ethanedithiol; **D**: trimethylolpropane tris(3-mercaptopropionate); **E**: pentaerythritol tetrakis(3-mercaptopropionate).

Initially, homopolymer P(EtOx)$_{10}$ was synthesized as the polymeric precursor **P1** (Table 1). Three different dithiol compounds (**A**, **B**, and **C**), a tri-thiol compound (**D**) and a tetra-thiol compound (**E**) have been investigated for the synthesis of extended linear (**P2–P4**) and star shaped polymers of PEtOx$_{10}$ (**P5–P6**). A DMF solvent system with TEA as a base was employed, as PFTR click reactions favor aprotic polar solvents and requires a non-nucleophilic base to mediate the nucleophilic attack process.[3,56–58] The mole ratio of [dithiol] : [PEtOx] : [Base] was selected as 1 : 2 : 2, where the mole ratio of PEtOx was calculated based on the mole amount of pentafluoro benzyl initiating group, with the concentration of dithiol A in DMF set at 1.0 M for solubility. Additionally, 0.5 mol% DMPP was added to prevent the formation of dithiol bridges. The coupling reaction was performed using a one-pot approach including the synthesis of corresponding P(EtOx) or P(EtOx-*b*-MeOx) precursors, which allows more precise measurement of initiator mole amount. The details of the one-pot synthesis procedure can be found in ESI.† PFTR click reactions were performed at room temperature as it has been proved efficient and convenient in our previous work.[55] A mixture of TEA, selected dithiol compound, and DMPP in DMF was added to the reaction mixture of PEtOx to start the click reaction. Samples were taken at different time points and SEC was employed to monitor the hydrodynamic volume change of samples. Obtained SEC results were collected in Fig. 3A–F and corresponding average molecular weights and dispersity values of obtained polymers were listed in Table 1. It was observed that for dithiol A and C in 2 hours the hydrodynamic volume of the polymer increased significantly, indicating the formation of diblock polymers. However, for dithiol B (Fig. 3B) only a small increase of hydrodynamic volume was observed after two hours. That might be the consequence of low nucleophilicity of the dithiol B, caused by the electronegative oxygen atom on the backbone, leading to a slow coupling reaction. Nevertheless, for dithiol B the increase of hydrodynamic volume was significant after 24 hours with no further increase seen after 48 hours, while the overlapped SEC trace suggesting significant amount of remaining unreacted **P1**.

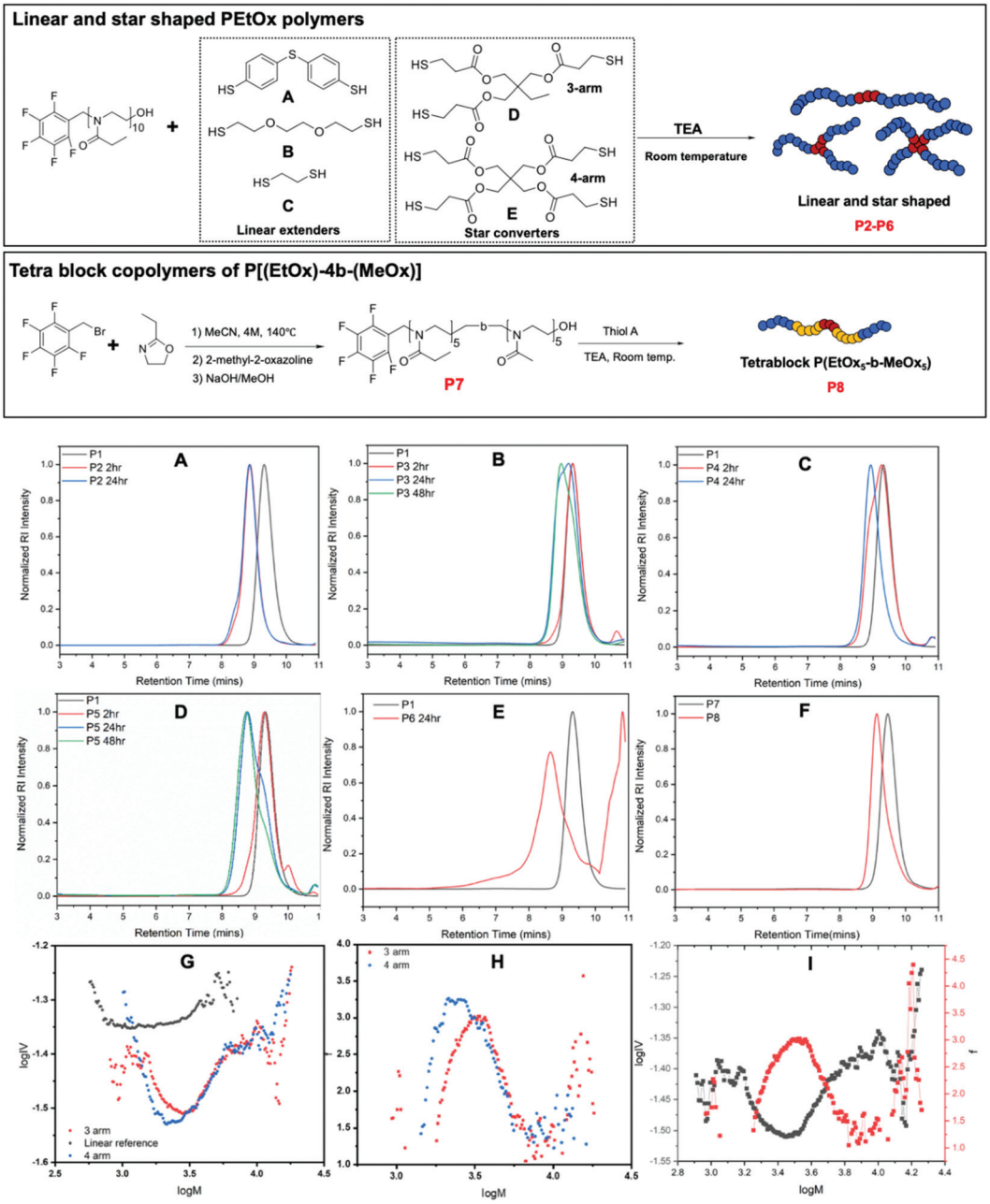

Fig. 3 Top: Reaction schemes for the synthesis of extended linear, star shaped, and tetrablock copolymers. Bottom SEC traces and advanced SEC analysis of extended linear, start shaped and tetrablock poly(2-oxazoline)s. (A–F) Corresponding SEC traces of PFTR coupling reaction of **P1**, **P7** with Thiols (A–E). (G–I) Viscosity analysis of 3-arm and 4-arm star polymers **P5** and **P6**, respectively. (G) Mark–Houwink plot for the 3 arm (**P5** in red) and 4 arm (**P6** in blue) star polymers formed *via* the PTFR click reaction. A reference PEtOx polymer **P1** is shown in black for comparison. (H) Functionality plot for both 3-arm and 4-arm star polymers showing how the number of arms varies with molar mass. Average number of arms was calculated for 3-arm and 4-arm star polymers, which are 2.2 and 2.3, respectively. (I) Overlapped Mark–Houwink plot and functionality plot of 3-arm star polymers showing the correspondence of decreased viscosity and increased number of arms.

This suggests that the reactions proceed albeit at a slower rate than dithiol A and the coupling efficiency might not be high. For dithiol C, a significant increase in hydrodynamic volume was observed after 2 hours but the overlay of SEC traces with **P1** suggests the coupling reaction was not complete (Fig. 3C). The complete shift of SEC trace was observed after 24 hours without any leftover homopolymers present.

3-Arm star polymer formation with thiol D (Fig. 3D) shows a small change in hydrodynamic volume after 2 hours, while a significant shift of the polymer peak was observed after 24 hours with a distorted curve shape that has a low molecular weight contribution. This indicates the presence polymer chains without a pentafluoro benzyl initiating group, or the trifunctional core did not fully react with pentafluoro benzyl

groups and thus generated 2-arm linear polymers. In the case of 4-arm star polymer formation with thiol E (Fig. 3E) significant increase of hydrodynamic volume was observed with after 24 hours with a tail present at high molecular weight. This might be the consequence of star-star coupling.

Preparation of block copolymers of EtOx and MeOx, PEtOx-*b*-MeOx, was also performed using PFBB as the initiator. The synthesis of block copolymers was monitored by ^{1}H NMR and SEC. Collected results were shown in ESI, Fig. S2.† This serves as the proof of concept of block copolymer synthesis of poly(2-oxazoline)s using PFBB as the initiator and adds potential for easy tetra block copolymer synthesis, which was then investigated, and corresponding SEC results were shown in Fig. 3F. A significant shift of polymer peaks indicating the coupling reaction was happening and generated tetrablock polymers, although the low molecular weight tailing in the SEC trace of **P8** suggesting the existence of unreacted diblock polymers. ^{1}H NMR and MALDI-ToF characterization results of the coupling reaction of PFB-PEtOx with dithiol A is displayed in the ESI (Fig. S3†). Analysis of the results for the coupling reaction of PFB-PEtOx with dithiol A has shown that the coupling reaction has a good efficiency as the major distribution in the MALDI-ToF MS that was close to the calculated theoretical molecular weight of the extended linear polymer (**P2**). Additionally, aromatic protons of dithiol C have been observed in the ^{1}H NMR and this along with the significant change in hydrodynamic volume in the SEC chromatogram support the creation of an extended linear polymer. The existence of other desired extended linear polymers (**P3** and **P4**) was proved by MALDI-ToF characterization and is shown in Fig. S4 and S5,† respectively. Unfortunately, it was not possible to obtain a MALDI-ToF MS analysis of the tetrablock polymer **P8** P($EtOx_5$-$MeOx_5$)$_2$-A; however, it was fully analyzed by ^{1}H NMR (Fig. S6†). It was noticeable that, although the SEC and ^{1}H NMR results indicate the success of coupling reactions, MALDI-ToF analysis of **P2** and **P4** show significantly deviated results with a difference between theoretical and experimental value of 3 to 7 Da. This indicates the current MALDI-ToF system, using dithranol or *trans*-2-[3-(4-*tert*-butylphenyl)-2-methyl-2-propenylidene] malononitrile (DCTB) as a matrix, sodium trifluoro acetate as a salt, and PMMA calibration standard, might not be the optimum system for analyzing these two polymers.

As the MALDI-ToF analysis of **P5** and **P6** did not provide a spectrum with acceptable signal-to-noise ratio, advanced SEC was employed to analyze obtained star polymers. Further analysis to study the degree of branching and number of arms of the obtained star polymers was performed using advanced SEC equipped with an RI and viscosity detectors. SEC viscosity analysis data for **P5** and **P6** are shown in Fig. 3G–I. Fig. 3G shows Mark–Houwink plot for both star polymers together with the linear reference polymer. Prior to any calculations for the number of arms is undertaken it is critical to qualitatively analyze the plots. This is because to obtain numerical values from intrinsic viscosity data an assumptive value for the structural factor, ε, is required. Firstly, if we consider the star polymer is prepared from a trifunctional core then the maximum number of arms would be 3 and that only a 1-arm, 2-arm or 3-arm structures are possible. Therefore, it can be assumed that the minima of viscosity represents 3-arm polymers because a 1-arm and 2-arm appear equivalent to a linear reference in a Mark–Houwink plot. However, there are data points between the reference and the minima which is due to co-elution. Here, co-elution is likely because the arms only have a theoretical molecular weight of 1000 Da whereas a 3-arm star has a theoretical molecular weight of 3000 Da meaning their hydrodynamic sizes are not significantly different. Thus, leftover arms, 1-arm and 2-arm polymers will co-elute with the star polymer and will lead to intrinsic viscosity (IV) values that are a weighted average of the species eluting. As will be shown later this leads to species that appear to have arms between 1–3 but this in reality is a mixture. In the same way we can qualitatively interpret the 4-arm star shaped polymer prepared from a tetrafunctional thiol core. The minima is slightly lower than that of the 3 arm star although this is not significant enough to suggest the formation of a 4 arm star polymer. However, given that it has a lower IV values than that of the 3 arm it is possible to infer that there is some degree of 4 arm species but that the presence of a 3 arm species increases the viscosity as a result of co-elution.

The number of arms, f, are estimated using the viscosity data and assuming a structural factor of 0.75.[59] With the assumption of a polydisperse system the arms were calculated and are shown in Fig. 3H. In keeping with the assessment previously provided the 3-arm star was found to have an average of 2.2 arms with a maximum of 3 arms. The 4-arm star was found to have an average of 2.3 arms and with a maximum of approximately 3.3 arms. As previously discussed, this implies that some 4 arm species is present to enable an average of 3.3. In Fig. 3I, the functionality plot and the Mark–Houwink plot of the 3-arm star was overlapped as an example to show the agreement between the viscosity and the number of arms, where the lowest viscosity point matches the highest number of arms. Overall, neither of the stars have a constant number of arms and the results show significant co-elution. It is worth noting that the results rely heavily on the structural factor being 0.75 which can vary,[60,61] as the structural factor ε would determine the relationship between radius of gyration contraction factor g and intrinsic viscosity contraction factor g'. Small deviations of this factor cause significant changes to the number of arms. In P. Guégan *et al.*, whereby they used a star-shaped initiator they used a method whereby the theoretical number of arms was considered in order to estimate a more accurate value for ε.[61] Considering the 3 arm polymer case where it is known that a maximum of 3 arms are possible the assumptive value for ε seems valid given that this is what the calculation and model used provided as an output.

Synthesis of multiblock PEtOx via PFTR and direct termination

The mechanism of PFTR click reaction has been discussed in several publications.[56,62,63] The nucleophilic attack of thiolate

ions to the *para*-fluorine has been reported as an important step in this *para*-fluoro-thiol click reaction (PFTR). The termination step in the synthesis of polyoxazoline involves the use of a nucleophile to attack the oxazolinium ion to end-cap the propagating chain. This stops the chain growth and installs functional groups on omega chain end. Various nucleophiles including amines, alcohols and thiolate salts have been reported to be utilized in the end-functionalization of polyoxazolines.[64] Both termination reaction of living chain ends and PFTR are highly efficient reactions. They require a nucleophilic attack and by polymerizing a 2-oxazoline with PFBB as the initiator, the living propagating chain could be treated as a A–B functionalized macromonomer. Thus, using a dithiol as a bi-nucleophile to simultaneously terminate living chain ends and take part in PFTCR could result in the preparation of multiblock oxazoline polymers in one-pot. It should also be noted that by using sequential addition of monomers to synthesis poly(2-oxazoline) block polymers, it is also possible to easily synthesize multiblock poly(2-oxazoline)s (Fig. 4).

In order to investigate the combination of cationic chain end termination with a thiol and performing *para*-fluoro thiol click reaction simultaneously, dithiol A was selected owing to relatively faster reaction kinetics of aromatic thiols. PEtOx with [monomer] to [initiator] molar ratio of 10 to 1 was synthesized

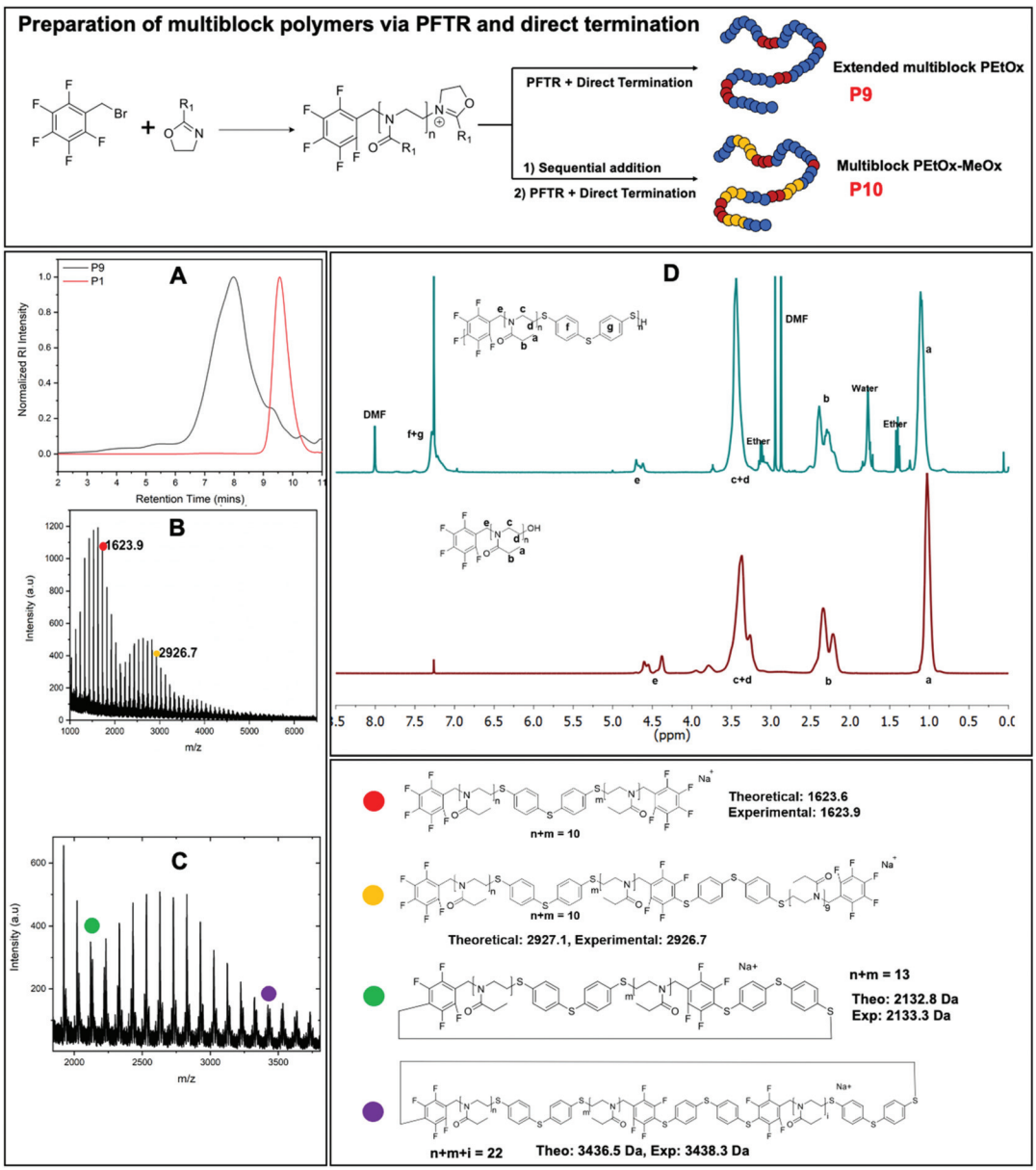

Fig. 4 Preparation of multiblock PEtOx and characterization of extended multiblock polymer **P9** with SEC (A), MALDI-ToF MS (B), zoom in to the high molar mass region in the MALDI-ToF MS (C), and ^{1}H NMR (D) showing the growth of multiblock polymer and possible cyclic structure formation (green and purple).

under microwave heating using PFBB as the initiator. The same reaction conditions were used as discussed in the kinetic study section. After 6 minutes of polymerization the reactor was cooled down to 40 °C with compress air. Then a vacuum dried and nitrogen degassed solution of dithiol A together with dry TEA and DMPP in dry DMF was added into the polymerization reaction. The molar ratio of reactants and base were kept at [Dithiol A] : [Initiator] : [TEA] : [DMPP] = 100 : 100 : 205 : 1.5. The reaction mixture was then heated for another 3 minutes at 70 °C. The obtained polymer (**P9**) was analyzed with ^{1}H NMR, SEC and MALDI-ToF MS. A significant increase of hydrodynamic volume and average molecular weight distribution were observed (Fig. 4A), indicating the formation of a multiblock PEtOx. Longer microwave heating did not lead to an increase in hydrodynamic volume, indicating that this was the full extent of reaction. The polymer was purified by precipitation in cold diethyl ether, filtration and drying in the vacuum oven. ^{1}H NMR analysis was carried out, which showed the presence of aromatic peaks indicative of the dithiol in the polymer backbone (Fig. 4D). MALDI-TOF MS spectra for the multiblock polymer (Fig. 4B) mainly shows peaks of low molecular weight, this is likely due to multiple aromatic and fluorinated aromatic rings making ionization of the polymer more difficult, and polymers with higher molar mass are known to be more difficult to ionize.[65–68] Nevertheless, observed values prove that the direct termination and the PFTR click reaction are both happening and resulting in polymer growth (Fig. 4B and C). For example, as shown in Fig. 4B the mass of peak observed at 1623.9 Da fits to the sodium salt of a diblock polymer with two pentafluoro benzyl end groups that are connected *via* the termination with dithiol A and have 10 EtOx repeating units in total. Additionally, the peak observed at 2926.7 Da fits to the value of the sodium salt of the polymer at 1623.9 Da having one aromatic dithiol reacted with one pentafluoro benzyl group, and the aromatic dithiol end-caps another PEtOx chain with 9 repeating units and a pentafluoro benzyl bromide group, indicates the mixed ways of chain growth presenting in the multiblock PEtOx formation. The zoom in analysis of secondary distributions (Fig. 4C) revealed potential cyclic structures formation as shown with two example peaks at 2133.3 Da and 3438.3 Da, which is an inevitable side reaction in step-growth polymerization. These results are suggesting the one-pot direct termination approach for preparing multiblock PEtOx was successful.

Based on the approach of synthesizing multiblock PEtOx with dithiol A, preparation of multiblock P(EtOx-*b*-MeOx) (**P10**) with dithiol A was performed using the same procedure. Similar results were obtained based on the ^{1}H NMR and SEC analysis. (Fig. S7†) The multiblock copolymer **P10** does not have a very large hydrodynamic volume change compared to the starting block polymer of PFB-P(EtOx-MeOx). A possible reason for this might be due to the chain end livingness of the P(EtOx-*b*-MeOx) that might be hampered while adding the second block, that changed the stoichiometry of step-growth polymerization and restricts the size of final polymer.

Self-assembly properties of amphiphilic polymer P2, P8, P9 and P10

The results discussed so far indicate that PFBB is a useful clickable initiator for the synthesis of desired diblock, star and multiblock polymers of PEtOx utilizing α-end and ω-end functionalities. Using a microwave assisted polymerization strategy, it is possible to obtain a multiblock P(EtOx-*b*-MeOx) in one pot in 10 minutes, which is very fast and convenient. Among obtained polymers, diblock polymer **P2**, tetrablock polymer **P8** and multiblock polymer **P9** and **P10** have an amphiphilic backbone structure with aromatic and fluorinated aromatic rings. Thus, the thermal responsive and self-assembly properties of these polymers were investigated. Surprisingly, no evidence for thermal responsiveness was found in THF. Moreover, these polymers were not soluble in water which is likely due to the presence of fluorinated and non-fluorinated aromatic rings within the backbone structure. The self-assembly behavior of these polymers is discussed in following section.

The self-assembly properties of **P2**, **P8**, **P9** and **P10** were investigated *via* a thin-film deposition approach. 5 mg of a corresponding polymer was dissolved in a 2.5 mL of 8 : 2 (v/v) THF/ether mixture to prepare a 2 mg mL^{-1} solution and then allowed to evaporate to prepare the polymer film. Distilled water was then added to the dried polymer film and stirred for 7 days to prepare nanoparticles. The prepared nanoparticle solution was filtered through a hydrophilic 0.2 micron PTFE filter to remove any kind of large aggregations and then characterized with TEM, which revealed that the architecture of polymer nanoparticles was predominantly spheres (Fig. 5) with diameters ranging from 184 nm to 250 nm. The diameters shown were obtained from the average value with the standard deviation of 15 different particles. The particles formed from these amphiphilic polymers showed a reasonable polydispersity. Particles of **P2**, the diblock polymer of PEtOx, are nanospheres but the size distribution is wide, while some particles of **P8**, the tetrablock polymer of PEtOx-MeOx, has distorted shape. As only one hydrophobic region presents in **P8**, the hydrophilicity difference of PEtOx and MeOx segment results in the shape distortion. The nanospheres formed form **P9**, the multiblock polymer of PEtOx, are the biggest in these four polymers as the chain length is also the longest. These nanospheres tend to aggregate, which might be a consequence of the presence of multiple aromatic rings in the polymer backbone which potentially allow the formation of π–π interactions which provide a driving force for aggregation. As the aggregation affects the measurement of nanoparticle size, only nanoparticles have a clear boundary like nanoparticle shown in Fig. 5, **P9** was measured to give the average value. Nanoparticles of **P10**, the multiblock polymer of PEtOx-MeOx, are spherical and more uniform in diameter comparing to other nanoparticles, indicating controlling the chain length to reduce the amount of aromatic rings might be helpful to prevent aggregation. It was also revealed that the nanoparticle solution of **P2**, **P8** and **P10** shown thermal triggered aggregation behavior, as indicated in Fig. 5. The transmittance

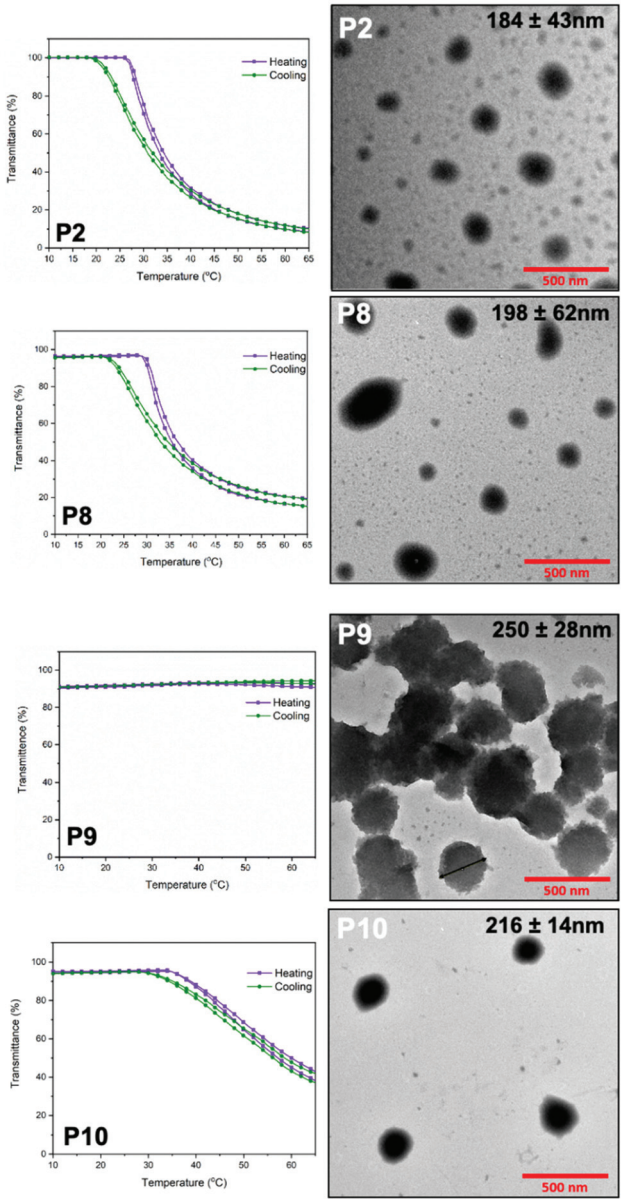

Fig. 5 Transmittance measurements at 550 nM (left) and TEM measurements (right) of **P2**, **P8**, **P9** and **P10**.

measurements obtained at 550 nm from 10 °C to 90 °C have shown that the reversible thermal aggregation of nanoparticle solutions of **P2**, **P8** and **P10** occurs in the temperature range of 25–35 °C, indicated by the decrease in transmittance value. The nanoparticle solution of **P9** did not show a thermal aggregation behavior, most likely due to longer chain length of **P9** that provides more hydrophilic POx chains and require larger thermodynamic driving force to aggregate. Obtained transmittance results also indicate the nanoparticle aggregation of **P9** observed in TEM possibly happened during the TEM sample preparation process. The self-assembly and thermal aggregation behaviors of these nanoparticle solutions show the importance of controlled chain length and dispersity to adjust the hydrophilicity of polymers to obtain nanoparticles that do not aggregate at a physiological temperature range.

Conclusions

In summary, 2,3,4,5,6-pentafluoro benzyl bromide was investigated as a clickable initiator for the cationic ring opening polymerization of 2-oxazoline copolymers and shown to be feasible not only for the controlled synthesis of PEtOx but also its further modification using *para*-fluoro-thiol click reaction. The utilization of a clickable pentafluoro benzyl group to synthesize extended linear, tetrablock and star polymers has been examined. Furthermore, we investigated the possibility of using a poly(2-oxazoline) with a pentafluoro benzyl group and utilizing the living chain end for the synthesis of multiblock polymers using a dithiol. Thus, poly(2-oxazoline) multiblock polymers were obtained and the self-assembly properties of obtained amphiphilic polymers were studied. Finally, poly(2-oxazoline) based nanoparticles sized from 184 nm to 250 nm were observed *via* TEM analysis. This work enriched the arsenal of clickable poly(2-oxazoline)s and provided access to preparation of different architecture of poly(2-oxazoline)s with a metal free, base catalyzed click reaction. As obtained multiblock polymers are not soluble in water, the partially hydrolysis of these polymers to adjust the hydrophilicity of multiblock polymers would be interesting future work as it might change the solubility as well as the self-assembly architecture of these polymers, and possibly produce useful polymers for drug delivery applications.

Author contributions

TZ has designed the project and performed the experiments, BD has contributed in the SEC analysis and GY has performed the TEM measurements. CRB has contributed in the design and supervision of the project.

Conflicts of interest

There are no conflicts to declare.

Acknowledgements

Authors are grateful to China Scholarship Council and University of Warwick for supporting TZ.

References

1 A. Tait, A. L. Fisher, T. Hartland, D. Smart, P. Glynne-Jones, M. Hill, E. J. Swindle, M. Grossel and D. E. Davies, Biocompatibility of poly(2-alkyl-2-oxazoline) brush surfaces for adherent lung cell lines, *Biomaterials*, 2015, **61**, 26–32.

2 M. N. Leiske, F. H. Sobotta, F. Richter, S. Hoeppener, J. C. Brendel, A. Traeger and U. S. Schubert, How To Tune the Gene Delivery and Biocompatibility of Poly(2-(4-aminobutyl)-2-oxazoline) by Self- and Coassembly, *Biomacromolecules*, 2018, **19**(3), 748–760.

3 K. Babiuch, R. Wyrwa, K. Wagner, T. Seemann, S. Hoeppener, C. R. Becer, R. Linke, M. Gottschaldt, J. Weisser, M. Schnabelrauch and U. S. Schubert, Functionalized, Biocompatible Coating for Superparamagnetic Nanoparticles by Controlled Polymerization of a Thioglycosidic Monomer, *Biomacromolecules*, 2011, **12**(3), 681–691.

4 T. Hayashi and A. Takasu, Design of electrophoretic and biocompatible poly(2-oxazoline)s initiated by perfluoroalkanesulfoneimides and electrophoretic deposition with bioactive glass, *Biomacromolecules*, 2015, **16**(4), 1259–1266.

5 T. Lorson, M. M. Lubtow, E. Wegener, M. S. Haider, S. Borova, D. Nahm, R. Jordan, M. Sokolski-Papkov, A. V. Kabanov and R. Luxenhofer, Poly(2-oxazoline)s based biomaterials: A comprehensive and critical update, *Biomaterials*, 2018, **178**, 204–280.

6 R. Luxenhofer, Y. Han, A. Schulz, J. Tong, Z. He, A. V. Kabanov and R. Jordan, Poly(2-oxazoline)s as polymer therapeutics, *Macromol. Rapid Commun.*, 2012, **33**(19), 1613–1631.

7 J. Tong, M. C. Zimmerman, S. Li, X. Yi, R. Luxenhofer, R. Jordan and A. V. Kabanov, Neuronal uptake and intracellular superoxide scavenging of a fullerene (C60)-poly(2-oxazoline)s nanoformulation, *Biomaterials*, 2011, **32**(14), 3654–3665.

8 R. W. Moreadith, T. X. Viegas, M. D. Bentley, J. M. Harris, Z. Fang, K. Yoon, B. Dizman, R. Weimer, B. P. Rae, X. Li, C. Rader, D. Standaert and W. Olanow, Clinical development of a poly(2-oxazoline) (POZ) polymer therapeutic for the treatment of Parkinson's disease – Proof of concept of POZ as a versatile polymer platform for drug development in multiple therapeutic indications, *Eur. Polym. J.*, 2017, **88**, 524–552.

9 S. C. Lee, S. W. K. C. Kim, I. C. Kwon and S. Y. Jeong, Synthesis and characterization of amphiphilic poly(2-ethyl-2-oxazoline)/poly(1-caprolactone) alternating multiblock copolymers, *Polymer*, 2000, (41), 7091–7097.

10 M. J. Isaacman, K. A. Barron and L. S. Theogarajan, Clickable Amphiphilic Triblock Copolymers, *J. Polym. Sci., Part A: Polym. Chem.*, 2012, **50**(12), 2319–2329.

11 M. W. M. Fijten, C. Haensch, B. M. van Lankvelt, R. Hoogenboom and U. S. Schubert, Clickable Poly(2-Oxazoline)s as Versatile Building Blocks, *Macromol. Chem. Phys.*, 2008, **209**(18), 1887–1895.

12 C. Diehl and H. Schlaad, Thermo-responsive polyoxazolines with widely tuneable LCST, *Macromol. Biosci.*, 2009, **9**(2), 157–161.

13 B. Guillerm, S. Monge, V. Lapinte and J.-J. Robin, Well-defined poly(oxazoline)-b-poly(acrylate) amphiphilic copolymers: From synthesis by polymer-polymer coupling to self-organization in water, *J. Polym. Sci., Part A: Polym. Chem.*, 2013, **51**(5), 1118–1128.

14 J. Kronek, Z. Kronekova, J. Luston, E. Paulovicova, L. Paulovicova and B. Mendrek, In vitro bio-immunological and cytotoxicity studies of poly(2-oxazolines), *J. Mater. Sci. Mater. Med.*, 2011, **22**(7), 1725–1734.

15 R. Luxenhofer, G. Sahay, A. Schulz, D. Alakhova, T. K. Bronich, R. Jordan and A. V. Kabanov, Structure-property relationship in cytotoxicity and cell uptake of poly(2-oxazoline) amphiphiles, *J. Controlled Release*, 2011, **153**(1), 73–82.

16 G. Morgese, S. N. Ramakrishna, R. Simic, M. Zenobi-Wong and E. M. Benetti, Hairy and Slippery Polyoxazoline-Based Copolymers on Model and Cartilage Surfaces, *Biomacromolecules*, 2018, **19**(2), 680–690.

17 B. Verbraeken, B. D. Monnery, K. Lava and R. Hoogenboom, The chemistry of poly(2-oxazoline)s, *Eur. Polym. J.*, 2017, **88**, 451–469.

18 T. Sezonenko, X.-P. Qiu, F. M. Winnik and T. Sato, Dehydration, Micellization, and Phase Separation of Thermosensitive Polyoxazoline Star Block Copolymers in Aqueous Solution, *Macromolecules*, 2019, **52**(3), 935–944.

19 O. Celebi, C. H. Lee, Y. Lin, J. E. McGrath and J. S. Riffle, Synthesis and characterization of polyoxazoline–polysulfone triblock copolymers, *Polymer*, 2011, **52**(21), 4718–4726.

20 B. Guillerm, S. Monge, V. Lapinte and J. J. Robin, How to modulate the chemical structure of polyoxazolines by appropriate functionalization, *Macromol. Rapid Commun.*, 2012, **33**(19), 1600–1612.

21 C. Giardi, V. Lapinte, F. Nielloud, J.-M. Devoisselle and J.-J. Robin, Synthesis of polyoxazolines using glycerol carbonate derivative and end chains functionalization via carbonate and isocyanate routes, *J. Polym. Sci., Part A: Polym. Chem.*, 2010, **48**(18), 4027–4035.

22 G. Delaittre, Telechelic poly(2-oxazoline)s, *Eur. Polym. J.*, 2019, **121**, 109281.

23 A. Krieg, C. Weber, R. Hoogenboom, C. R. Becer and U. S. Schubert, Block Copolymers of Poly(2-oxazoline)s and Poly(meth)acrylates: A Crossover between Cationic Ring-Opening Polymerization (CROP) and Reversible Addition–Fragmentation Chain Transfer (RAFT), *ACS Macro Lett.*, 2012, **1**(6), 776–779.

24 B. Golba, E. M. Benetti and B. G. De Geest, Biomaterials applications of cyclic polymers, *Biomaterials*, 2021, **267**, 120468.

25 L. Trachsel, M. Romio, S. N. Ramakrishna and E. M. Benetti, Fabrication of Biopassive Surfaces Using Poly (2-alkyl-2-oxazoline)s: Recent Progresses and Applications, *Adv. Mater. Interfaces*, 2020, **7**(19), 2000943.

26 M. Schroffenegger, N. S. Leitner, G. Morgese, S. N. Ramakrishna, M. Willinger, E. M. Benetti and E. Reimhult, Polymer Topology Determines the Formation of Protein Corona on Core–Shell Nanoparticles, *ACS Nano*, 2020, **14**(10), 12708–12718.

27 M. N. Leiske, M. Lai, T. Amarasena, T. P. Davis, K. J. Thurecht, S. J. Kent and K. Kempe, Interactions of core cross-linked poly(2-oxazoline) and poly(2-oxazine) micelles with immune cells in human blood, *Biomaterials*, 2021, **274**, 120843.

28 A. K. Blakney, G. Yilmaz, P. F. McKay, C. R. Becer and R. J. Shattock, One Size Does Not Fit All: The Effect of Chain Length and Charge Density of Poly(ethylene imine) Based Copolymers on Delivery of pDNA, mRNA, and RepRNA Polyplexes, *Biomacromolecules*, 2018, **19**(7), 2870–2879.

29 M. J. Sanchez-Fernandez, M. R. Immers, R. P. Felix Lanao, F. Yang, J. Bender, J. Mecinovic, S. C. G. Leeuwenburgh and J. C. M. van Hest, Alendronate-Functionalized Poly(2-oxazoline)s with Tunable Affinity for Calcium Cations, *Biomacromolecules*, 2019, **20**(8), 2913–2921.

30 K. Kempe, S. Onbulak, U. S. Schubert, A. Sanyal and R. Hoogenboom, pH degradable dendron-functionalized poly(2-ethyl-2-oxazoline) prepared by a cascade "double-click" reaction, *Polym. Chem.*, 2013, **4**(11), 3236–3244.

31 C. A. Fustin, H. Huang, R. Hoogenboom, F. Wiesbrock, A. M. Jonas, U. S. Schubert and J. F. Gohy, Evaporation induced micellization of poly(2-oxazoline) multiblock copolymers on surfaces, *Soft Matter*, 2006, **3**(1), 79–82.

32 R. Aksakal, M. Resmini and C. R. Becer, Pentablock star shaped polymers in less than 90 minutes via aqueous SET-LRP, *Polym. Chem.*, 2016, **7**(1), 171–175.

33 T. Kaname, K. Aoi and O. Masahiko, Synthesis of Polyoxazoline-(Glyco)peptide Block Copolymers by Ring-Opening Polymerization of (Sugar-Substituted) R-Amino Acid N-Carboxyanhydrides with Polyoxazoline Macroinitiators, *Macromolecules*, 1997, **30**, 4013–4017.

34 X. Pan, Y. Liu, Z. Li, S. Cui, H. Gebru, J. Xu, S. Xu, J. Liu and K. Guo, Amphiphilic Polyoxazoline-block-Polypeptoid Copolymers by Sequential One-Pot Ring-Opening Polymerizations, *Macromol. Chem. Phys.*, 2017, **218**(6), 1600483.

35 B. A. Drain and C. R. Becer, Synthetic approaches on conjugation of poly(2-oxazoline)s with vinyl based polymers, *Eur. Polym. J.*, 2019, **119**, 344–351.

36 B. A. Drain, V. P. Beyer, B. Cattoz and C. R. Becer, Solvent Dependency in the Synthesis of Multiblock and Cyclic Poly(2-oxazoline)s, *Macromolecules*, 2021, **54**(12), 5549–5556.

37 C. R. Becer, R. M. Paulus, S. Höppener, R. Hoogenboom, C.-A. Fustin, J.-F. Gohy and U. S. Schubert, Synthesis of Poly(2-ethyl-2-oxazoline)-b-poly(styrene) Copolymers via a Dual Initiator Route Combining Cationic Ring-Opening Polymerization and Atom Transfer Radical Polymerization, *Macromolecules*, 2008, **41**(14), 5210–5215.

38 K. Kempe, A. Krieg, C. R. Becer and U. S. Schubert, "Clicking" on/with polymers: a rapidly expanding field for the straightforward preparation of novel macromolecular architectures, *Chem. Soc. Rev.*, 2012, **41**(1), 176–191.

39 U. Mansfeld, C. Pietsch, R. Hoogenboom, C. R. Becer and U. S. Schubert, Clickable initiators, monomers and polymers in controlled radical polymerizations – a prospective combination in polymer science, *Polym. Chem.*, 2010, **1**(10), 1560–1598.

40 K. Lava, B. Verbraeken and R. Hoogenboom, Poly(2-oxazoline)s and click chemistry: A versatile toolbox toward multifunctional polymers, *Eur. Polym. J.*, 2015, **65**, 98–111.

41 R. L. a. R. Jordan, Click Chemistry with Poly(2-oxazoline)s, *Macromolecules*, 2006, **39**(10), 3509–3516.

42 C. von der Ehe, K. Kempe, M. Bauer, A. Baumgaertel, M. D. Hager, D. Fischer and U. S. Schubert, Star-Shaped Block Copolymers by Copper-Catalyzed Azide-Alkyne Cycloaddition for Potential Drug Delivery Applications, *Macromol. Chem. Phys.*, 2012, **213**(20), 2146–2156.

43 K. Kempe, K. L. Killops, J. E. Poelma, H. Jung, J. Bang, R. Hoogenboom, H. Tran, C. J. Hawker, U. S. Schubert and L. M. Campos, Strongly Phase-Segregating Block Copolymers with Sub-20 nm Features, *ACS Macro Lett.*, 2013, **2**(8), 677–682.

44 T. Loontjens and L. Rique-Lurbet, Synthesis of α-alkyl ω-trimethoxysilane polyoxazolines and their application as coatings on glass fibres, *Des. Monomers Polym.*, 2012, **2**(3), 217–229.

45 C. R. Becer, R. Hoogenboom and U. S. Schubert, Click chemistry beyond metal-catalyzed cycloaddition, *Angew. Chem., Int. Ed. Engl.*, 2009, **48**(27), 4900–4908.

46 C. Alexis, C. Charnay, V. Lapinte and J.-J. Robin, Hydrophilization by coating of silylated polyoxazoline using sol–gel process, *Prog. Org. Coat.*, 2013, **76**(4), 519–524.

47 M. J. Isaacman, E. M. Corigliano and L. S. Theogarajan, Stealth polymeric vesicles via metal-free click coupling, *Biomacromolecules*, 2013, **14**(9), 2996–3000.

48 M. Hartlieb, T. Floyd, A. B. Cook, C. Sanchez-Cano, S. Catrouillet, J. A. Burns and S. Perrier, Well-defined hyperstar copolymers based on a thiol–yne hyperbranched core and a poly(2-oxazoline) shell for biomedical applications, *Polym. Chem.*, 2017, **8**(13), 2041–2054.

49 E. M. Wilts and T. E. Long, Thiol–ene addition enables tailored synthesis of poly(2−oxazoline)–graft–poly(vinyl pyrrolidone) copolymers for binder jetting 3D printing, *Polym. Int.*, 2020, **69**(10), 902–911.

50 J. F. Nawroth, J. R. McDaniel, A. Chilkoti, R. Jordan and R. Luxenhofer, Maleimide-Functionalized Poly(2-Oxazoline)s and Their Conjugation to Elastin-Like Polypeptides, *Macromol. Biosci.*, 2016, **16**(3), 322–333.

51 M. W. M. Fijten, R. Hoogenboom and U. S. Schubert, Initiator effect on the cationic ring-opening copolymerization of 2-ethyl-2-oxazoline and 2-phenyl-2-oxazoline, *J. Polym. Sci., Part A: Polym. Chem.*, 2008, **46**(14), 4804–4816.

52 R. Hoogenboom, M. W. M. Fijten, H. M. L. Thijs, B. M. van Lankvelt and U. S. Schubert, Microwave-assisted synthesis and properties of a series of poly(2-alkyl-2-oxazoline)s, *Des. Monomers Polym.*, 2012, **8**(6), 659–671.

53 R. M. Paulus, C. R. Becer, R. Hoogenboom and U. S. Schubert, Acetyl Halide Initiator Screening for the Cationic Ring-Opening Polymerization of 2-Ethyl-2-Oxazoline, *Macromol. Chem. Phys.*, 2008, **209**(8), 794–800.

54 K. Matyjaszewski, The importance of exchange reactions in controlled/living radical polymerization in the presence of alkoxyamines and transition metals, *Macromol. Symp.*, 1996, **111**(1), 47–61.

55 T. Zhao, V. P. Beyer and C. R. Becer, Fluorinated Polymers via Para-Fluoro-Thiol and Thiol-Bromo Click Step Growth Polymerization, *Macromol. Rapid Commun.*, 2020, **41**(22), e2000409.
56 G. Delaittre and L. Barner, The para-fluoro-thiol reaction as an efficient tool in polymer chemistry, *Polym. Chem.*, 2018, **9**(20), 2679–2684.
57 C. R. Becer, K. Babiuch, D. Pilz, S. Hornig, T. Heinze, M. Gottschaldt and U. S. Schubert, Clicking Pentafluorostyrene Copolymers: Synthesis, Nanoprecipitation, and Glycosylation, *Macromolecules*, 2009, **42**(7), 2387–2394.
58 C. R. Becer, K. Kokado, C. Weber, A. Can, Y. Chujo and U. S. Schubert, Metal-free synthesis of responsive polymers: Cloud point tuning by controlled "click" reaction, *J. Polym. Sci., Part A: Polym. Chem.*, 2010, **48**(6), 1278–1286.
59 M. Bohdanecky, A Semiempirical Formulation of the Effect of Random Branching on Intrinsic Viscosity, *Macromolecules*, 1977, **10**, 971–975.
60 S. T. Balke, T. H. Mourey, D. R. Robello, T. A. Davis, A. Kraus and K. Skonieczny, Quantitative analysis of star-branched polymers by multidetector size-exclusion chromatography, *J. Appl. Polym. Sci.*, 2002, **85**(3), 552–570.
61 L. Plet, G. Delecourt, M. Hanafi, N. Pantoustier, G. Pembouong, P. Midoux, V. Bennevault and P. Guégan, Controlled star poly(2-oxazoline)s: Synthesis, characterization, *Eur. Polym. J.*, 2020, **122**, 109323.
62 N. H. Park, G. D. P. Gomes, M. Fevre, G. O. Jones, I. V. Alabugin and J. L. Hedrick, Organocatalyzed synthesis of fluorinated poly(aryl thioethers), *Nat. Commun.*, 2017, **8**(1), 166.
63 J. Engelke and V. X. Truong, Visible light enabled para-fluoro-thiol ligation, *Polym. Chem.*, 2020, **11**(44), 7015–7019.
64 M. Glassner, M. Vergaelen and R. Hoogenboom, Poly(2-oxazoline)s: A comprehensive overview of polymer structures and their physical properties, *Polym. Int.*, 2018, **67**(1), 32–45.
65 L. Przybilla, J.-D. Brand, K. Yoshimura, H. J. Rader and K. Mullen, MALDI-TOF Mass Spectrometry of Insoluble Giant Polycyclic Aromatic Hydrocarbons by a New Method of Sample Preparation, *Anal. Chem.*, 2000, **72**, 4591–4597.
66 J. Zhang, X. Dong, J. Cheng, J. Li and Y. Wang, Efficient analysis of non-polar environmental contaminants by MALDI-TOF MS with graphene as matrix, *J. Am. Soc. Mass Spectrom.*, 2011, **22**(7), 1294–1298.
67 A. Baumgaertel, C. R. Becer, M. Gottschaldt and U. S. Schubert, MALDI-TOF MS Coupled with Collision-Induced Dissociation (CID) Measurements of Poly(methyl methacrylate), *Macromol. Rapid Commun.*, 2008, **29**(15), 1309–1315.
68 A. C. Crecelius, C. R. Becer, K. Knop and U. S. Schubert, Block length determination of the block copolymer mPEG-b-PS using MALDI-TOF MS/MS, *J. Polym. Sci., Part A: Polym. Chem.*, 2010, **48**(20), 4375–4384.